Interaction of Hydrated Protons with Trioctylphosphine Oxide: NMR and Theoretical Study

Jaroslav Kříž,*,† Jiří Dybal,† Emanuel Makrlík,‡ Jan Budka,§ and Petr Vaňura§

Institute of Macromolecular Chemistry AS CR, v. v. i., Heyrovského Sq. 2, 162 06 Prague, Czech Republic, Faculty of Applied Sciences, University of West Bohemia, Husova 11, 306 14 Pilsen, Czech Republic, and Prague Institute of Chemical Technology, Technická 5, 166 28 Prague, Czech Republic

Received: February 11, 2009; Revised Manuscript Received: April 7, 2009

Interaction of trioctylphosphine oxide (TOPO) with fully ionized hydrated protons (HP) was studied in acetonitrile-d_3 and nitrobenzene-d_5 using ^{1}H, ^{13}C, and ^{31}P NMR, PFG NMR, and magnetic relaxation, and the experimental results were confronted with high-precision ab initio DFT calculations. Relative chemical shifts of NMR signals of TOPO (0.02 mol/L) under the presence of HP in the molar ratio $\beta = 0-2.0$ mol/mol show binding between TOPO and HP. Self-diffusion measurements using ^{1}H PFG NMR demonstrate that larger complexes with higher content of TOPO are generally formed at $\beta < 0.75$. Analyzing the dependence of ^{31}P NMR chemical shifts on β by the use of program LETAGROP, we obtained very good fitting for the assumed coexistence of three complexes $(TOPO)_i \cdot HP$ (named C_i), where $i = 1, 2, 3$. The logarithms of the respective stabilization constants log K_i were found to be 3.63, 4.67, and 7.23 in acetonitrile and 3.91, 6.04, and 7.92 in nitrobenzene. The ^{31}P NMR chemical shifts $\Delta\delta_i$ corresponding to these complexes are 39.35, 29.51, and 19.72 ppm in acetonitrile and 38.37, 28.47, and 18.63 ppm in nitrobenzene. These values and the calculated values of $\alpha_i = [C_i]/[TOPO]_0$ were utilized in the analysis of the system dynamics. This was done by measuring the transverse ^{31}P NMR relaxation by the CPMG sequence with varying delays t_p between the π pulses in the mixtures with $\beta = 0.5$, 1.25, and 1.5. Calculating the probabilities of imaginable exchange processes shows that only three of them can have significant influence on relaxation rate R_2, namely $C_1 \leftrightarrow$ TOPO, $C_2 \leftrightarrow C_1$, and $C_3 \leftrightarrow C_2$. Using the slopes of the $R_2 - t_p^{-1}$ dependences in the above three mixtures, the following correlation times were obtained: $\tau_{10} = 2.5 \times 10^{-6}$, $\tau_{21} = 7.4 \times 10^{-5}$, $\tau_{32} = 11.3 \times 10^{-5}$ s. The DFT calculations support the hypothesis that complexes C_1 to C_3 are the main species in the mixtures of TOPO with HP, with the only exception that additional water molecules are bound to the complexes in the case of C_1 and C_2. Schematically, the compositions of the three stable complexes is $[3TOPO \cdot H_3O]^+$, $[2TOPO \cdot H_3O \cdot H_2O]^+$, and $[TOPO \cdot H_3O \cdot 2H_2O]^+$. The relative ^{31}P NMR shifts calculated for the optimized structures of C_1, C_2, and C_3 are in very good agreement with the experimentally observed values.

Introduction

Many compounds have been investigated as complexing agents and effective carriers of metallic cations in organic media, with various intentions such as extracting rare metals, devising catalytic systems or modeling cation receptors on cells, etc. Some of them, like modified calixarenes[1−11] or crown ethers,[12−14] owe their complexing ability to a more or less fixed configuration of several electron-donor groups forming electrostatic bonds with the cation. In all these cases, strong binding of protons in various hydrated states (referred to further as hydrated protons, HP) was found, too. Instead of pure electrostatic attraction, hydrogen bonding was proved to be the main interaction. In modified calixarenes, both typical coordinating groups (such as carbonyl, amide, thioamide, and ester groups) and phenoxy-oxygen atoms were utilized[15−19] as hydrogen bond acceptors; in crown ethers, the ether oxygen atoms were proved do play this role.[20−27] There were always at least three or four strong hydrogen bonds involved in the stabilization of the corresponding complex.

However, there are also complexing agents with only one but strongly basic group. One of the most popular in radiochemistry (as extraction agent) but also in synthetic chemistry (for preparing quantum dots, various sensors, and membranes) is trioctylphosphine oxide (TOPO), which was shown to bind with various metallic cations.[28−37] In most of the corresponding complexes, however, TOPO is mixed with other ligands and almost no data are available about their detailed structure or stability. No study to our knowledge was done on the interaction of TOPO with protons or HP. This lack is rather serious considering that most extractions of radioactive or rare elements are done in highly acidic media where HP can compete in binding with the incident metallic ion.

The ability of TOPO to bind HP (H_3O^+ or higher proton hydrates) is highly probable considering the electronic properties of the trialkyl-substituted P═O group. However, there is no information in the literature if any stable complex of TOPO with HP can be observed and, consequently, about its stability and structure. In principle, many possible structures can be imagined starting with $[TOPO_3 \cdot H_3O]^+$ or $[TOPO_4 \cdot H_5O_2]^+$ and proceeding with various other complexes with lower TOPO/proton ratios. The interest in the actual structures and their stability is both practical, as indicated above, and theoretical, as TOPO is a representative of a class of monofunctional

* To whom correspondence should be addressed. E-mail: kriz@imc.cas.cz. Phone: +420-296809382. Fax: +420-296809410.
† Institute of Macromolecular Chemistry.
‡ University of West Bohemia.
§ Prague Institute of Chemical Technology.

10.1021/jp9012575 CCC: $40.75
Published on Web 04/23/2009

SCHEME 1: Structure of HDCC

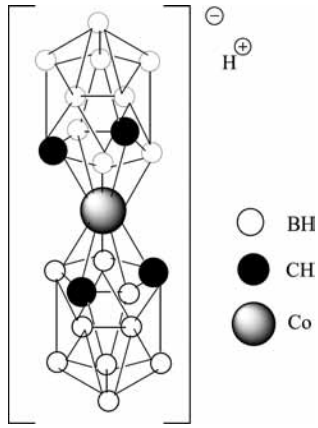

ligands, which can bind with cations but usually do not form very stable complexes.

As in most our previous approaches,[15−19,26,27] we performed the present study of interaction between TOPO and HP in relatively polar organic media (nitrobenzene and acetonitrile) ascertaining ionization by their dielectric constant ($\varepsilon > 35$). As a reliable source of well-ionized protons,[38] hydrogen bis(1,2-dicarbollyl) cobaltate (HDCC, see Scheme 1) was used. In our experiments, HDCC contained 3.5 mol/mol of H_2O per one proton due to which HP in various hydration states up to $H_7O_3^+$ could be present.

Experimental Section

Materials and Samples. Trioctylphosphine oxide (TOPO) was purchased from Sigma-Aldrich in reagent-plus grade and used as obtained. Hydrogen bis(1,2-dicarbollyl) cobaltate (HDCC) was prepared from cesium bis(1,2-dicarbollyl) cobaltate (HDCC) by the method published elsewhere[38] and dried under vacuum for several weeks. In its final state, it still contained 3.5 mol of H_2O per 1 mol of HDCC. Nitrobenzene-d_5 and acetonitrile-d_3 were purchased from Sigma-Aldrich and dried over a molecular sieve before use. All samples for NMR measurements contained 20 mmol/L of TOPO and various amounts of HDCC dissolved in nitrobenzene-d_5 or acetonitrile-d_3. The samples were stored and measured at 296 K.

NMR Spectra. ^{1}H, ^{13}C, and ^{31}P NMR spectra were measured at 300.13, 75.45, and 121.44 MHz, respectively, with an upgraded Bruker Avance DPX300 spectrometer. A total of 32 and 64 kpoints were measured for ^{1}H and ^{13}C NMR, respectively. ^{13}C NMR measurements were performed using the ^{1}H−^{13}C DEPT45 sequence (collecting 6000 scans). Basic ^{31}P NMR spectra were measured using a single-pulse sequence with WALTZ decoupling during acquisition; usually, 128 or 256 scans were collected. Exponential weighting (lb = 1 Hz) was used before Fourier transform in both ^{13}C and ^{31}P NMR. For the fitting of the dependences of the ^{31}P NMR chemical shift on the β = HDCC/TOPO ratio to the equilibrium constants the program[39] LETAGROP was used. For the exchange dynamics, the Carr−Purcell−Meiboom−Gill sequence[40−42] was used on the ^{31}P NMR resonance with the delay between π pulses t_p being 2.0, 1.0, 0.5, 0.25, and 0.125 ms (the length of the π pulse was 26.8 μs). A total of 32 experimental points with the total time of the sequence gradually increased by 40 ms were measured in one experiment with the given t_p. Each measurement was repeated at least three times. The error of the obtained R_2 was lower than 3% rel. Pulsed-field-gradient stimulated-echo (PGSTE) experiments[43,44] for measuring the diffusion coefficient were done on the ^{1}H NMR resonance using a water-cooled gradient probe and Bruker gradient unit; the diffusion delay was held constant (20 ms) and the field gradient was incremented in 16 steps in the range 0−200 G/cm.

Quantum Mechanical Calculations. Molecular orbital calculations were performed using the GAUSSIAN 03 suite of programs.[45] The molecular geometry was fully optimized at the B3LYP level of density functional theory (DFT) with the 6-31G(d) basis set. The optimization was unrestrained; vibrational frequencies were used to characterize the stationary points as minima. Several local configurations near the achieved energy minimum were examined. As the renewed optimizations converged to the same molecular geometry, we believe the achieved energy minimum to be the global one. The GIAO (gauge including atomic orbitals) method with the 6-311+G(2d,p) basis set was used to calculate NMR parameters. ^{31}P chemical shifts (in ppm) were calculated using H_3PO_4 as the reference.

Results and Discussion

Due to the presence of 3.5 mol of H_2O per every mol of HDCC, hydrates $H^+ \cdot nH_2O$ with n from 1 to 3 or 4 were possible. Although the water molecules that build up these hydrates can in principle compete with TOPO in the interaction with protons, the following results show that the situation is different. H_3O^+ is, usually in a slightly modified form, the building block of all TOPO complexes. Further water molecules are attached to the bound H_3O^+, providing that there are sites free for hydrogen bonding. They cannot effectively compete with TOPO. As there is always enough water in the system to form H_3O^+ quantitatively from the protons, which in turn are quantitatively provided by HDCC, we can identify HP with H_3O^+ and assume their initial concentration to be that of HDCC. In the following, the quantity β means the molar ratio $\beta = [HP]_0/[TOPO]_0 \equiv [HDCC]_0/[TOPO]_0$.

NMR Evidence of the Interaction of TOPO with HP. Like in other cases of organic molecules strongly interacting with HP, the complex-forming has a clear reflection in the change of the corresponding NMR spectra. ^{1}H and ^{13}C NMR spectra of two extreme mixtures are shown in Figures 1 and 2, respectively. The signals are assigned according to the numbering the carbon (or attached proton) atoms progressively according to their increasing distance from the P═O group. Although the spectra are somewhat obscured by the strong spin coupling of the ^{1}H and ^{13}C nuclei to the ^{31}P nucleus (and additional coupling between the vicinal protons in ^{1}H NMR spectra), one can clearly see two main features of the spectral changes: (i) There are marked relative shifts of the signals of almost all nuclei of the mutually equivalent octyl groups, which are about 0.53 ppm downfield for the protons 1 and about 4.1 ppm upfield for the corresponding carbon. The shifts point, in both their direction and magnitude, to a pronounced decrease in electron density in the valence orbitals of phosphorus. Thus strong hydrogen bonding of hydrated proton to the P═O group must take place. As one can expect, considering the low permeability of an aliphatic chain to electron perturbations, the relative shifts of both protons and carbons decrease with increasing distance of the respective nucleus from the P═O group. (ii) It can be shown (not demonstrated here for ^{1}H and ^{13}C because a much more illustrative case for ^{31}P is given below) that the signals gradually shift when increasing the value of β (up to some limiting value about 2) retaining their multiplicity and number. This means that a fast exchange between the free molecule of TOPO and its bound form (or forms) takes place, under which the actual chemical shift of the given signal is a weighted mean of those of the exchanging forms. Such a fast exchange is not

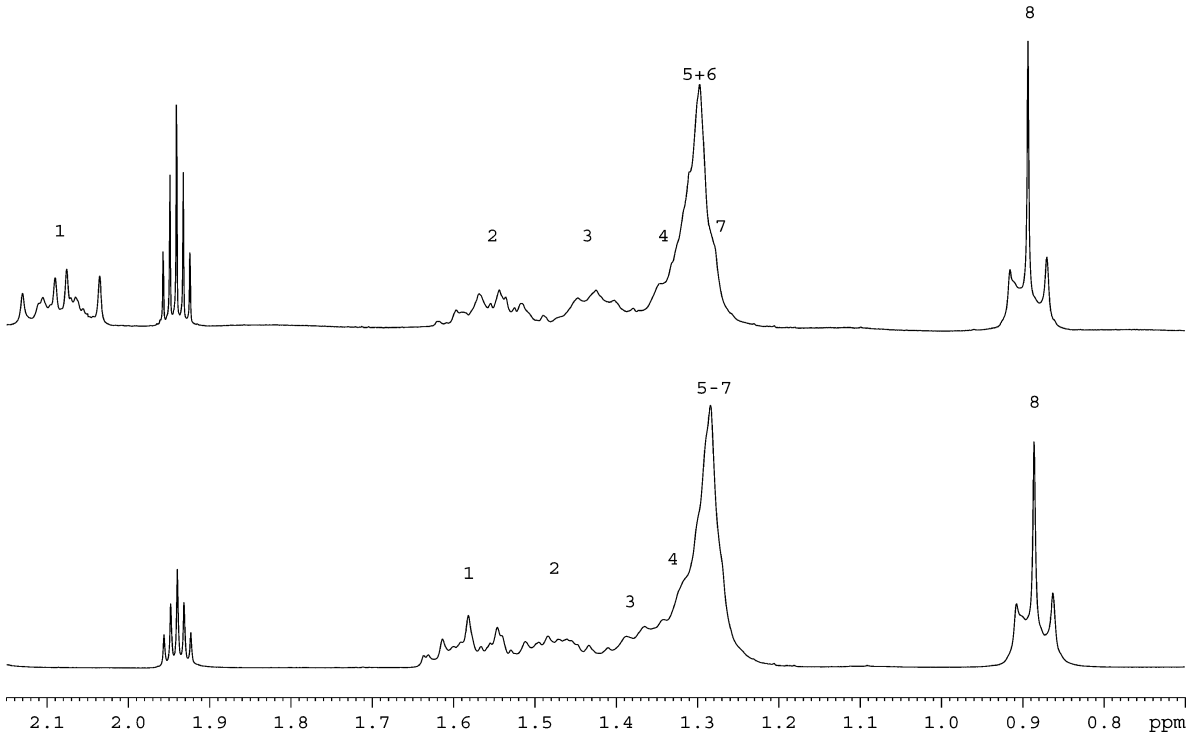

Figure 1. 300.13 MHz ^{1}H NMR spectra of a 0.02 mol/L solution of TOPO in acetonitrile-d_3 (bottom) and its mixture with 0.04 mol/L of HDCC (top) at 296 K.

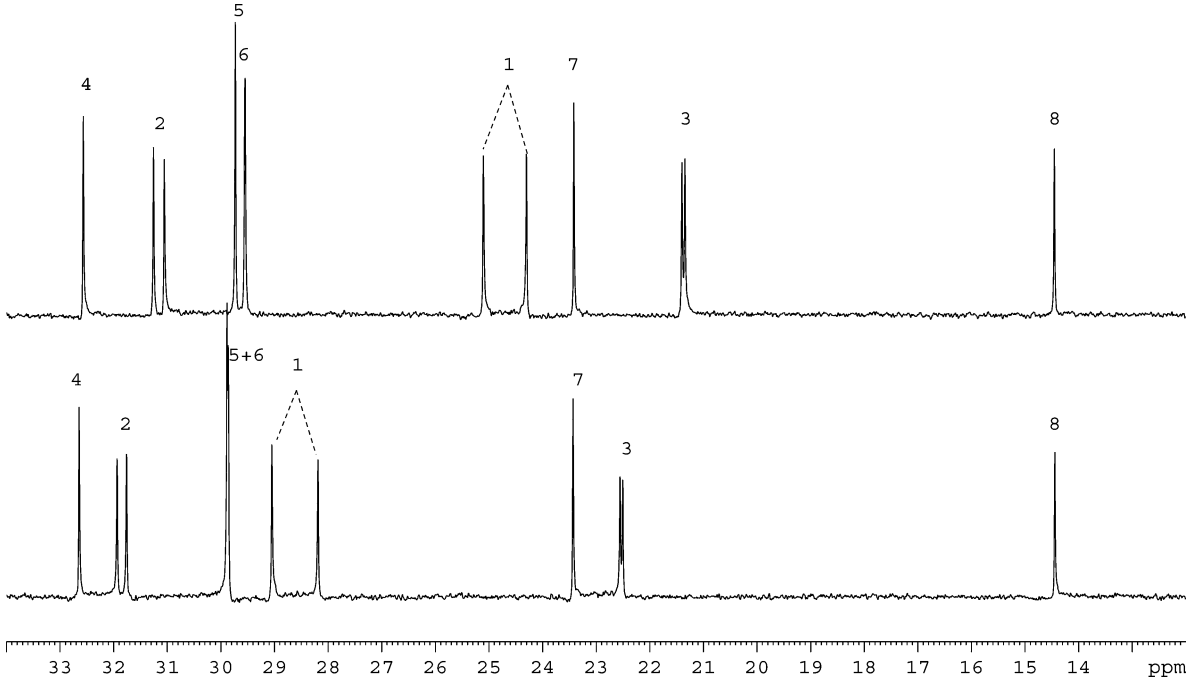

Figure 2. 75.45 MHz ^{13}C NMR DEPT45 spectra of a 0.02 mol/L solution of TOPO in acetonitrile-d_3 (bottom) and its mixture with 0.04 mol/L of HDCC (top) at 296 K.

very surprising, as we observed it even with the HP embedded into many-sited molecules like calixarenes or crown-ethers.[15−19,26,27]

A very illustrative reflection of the exchange can be seen in Figure 3 containing the gradual development of ^{31}P NMR spectra, this time in nitrobenzene-d_5 (in acetonitrile-d_3, the pattern is quite analogous). As one can see, the largest relative downfield shift between free and final bound forms of TOPO is about 40 ppm in acetonitrile-d_3 and 37.9 ppm in nitrobenzene-d_5. Again, the ^{31}P NMR signal of TOPO gradually shifts with increasing β up to about 2 without splitting, complying thus with the hypothesis of fast exchange between bound and free forms of TOPO. However, the pattern of the signal shape development with increasing β is rather remarkable: we observe intensive broadening at β below 0.3, above which the signal somewhat narrows, broadening again near $\beta = 0.75$ and gradually narrowing at higher β. At $\beta = 2$, the signal is as narrow as that of free TOPO in its original solution. The most probable cause of the signal broadening is the slowing-down of exchange. As there are two concentration regions of such slowing-down, there must be at least two forms of TOPO−HP

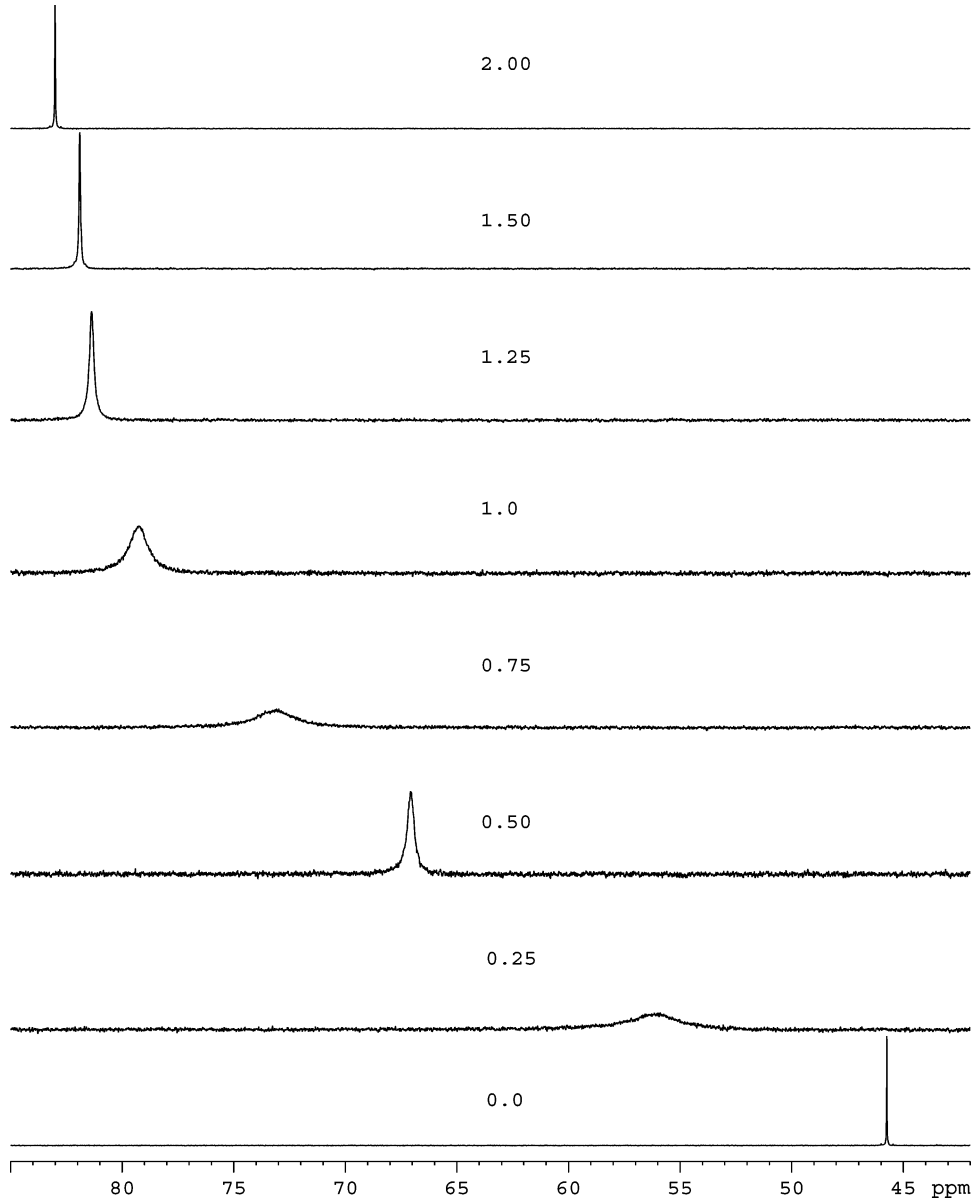

Figure 3. ^{31}P NMR spectra of the mixtures of a 0.02 mol/L TOPO with HDCC (molar ratio β indicated) in nitrobenzene-d_5 at 296 K.

complex at play. Considering that the simplest form of HP, the hydronium ion H_3O^+, offers three sites for a strong hydrogen bond with TOPO, we conjectured that there are three main forms in the system: [3TOPO·HP] (C_3), [2TOPO·HP] (C_2), and [TOPO·HP] (C_1). Below, it is shown that this conjecture agrees well with the chemical shift fitting as well as with the analysis of dynamics.

It is evident that HP cannot be the same in C_3, C_2, and C_1; with some approximation, one can identify it with H_3O^+, $H_3O^+ \cdot H_2O$, and $H_3O^+ \cdot 2H_2O$, respectively. The pattern of the signal development could be explained if C_3 is preferentially formed at low HP concentration and its exchange with free TOPO is only medium-fast; at somewhat higher HP concentrations, exchange between C_3 + HP and C_2 should have a slightly higher rate; finally, exchange between C_2 + HP and C_1 should be the fastest. It is evident that this is a simplified scheme; for instance, both C_2 and C_1 certainly could exchange with free TOPO. Further discussion of the dynamics is below in a separate paragraph.

PFG NMR Measurements. If the exchange between free TOPO and its various bound forms is fast enough, the gradient-dependent decay of the exchange-averaged signal in a pulsed field gradient stimulated echo (PGSTE) NMR spectrum should be monoexponential and the resulting self-diffusion coefficient should be a weighted average of the coefficients of individual mutually exchanging forms. Assuming that those forms are TOPO and C_3, C_2, and C_1 introduced in the previous paragraph, the following relation should hold for the apparent diffusion coefficient D:

$$D = (1 - \sum_{i=1}^{3} \alpha_i) D_0 + \sum_{i=1}^{3} \alpha_i D_i \qquad (1)$$

where D_0 is the diffusion coefficient of the free TOPO and the others D_i (i = 1, 2, 3) are those of the binding forms C_i; $\alpha_i = i[C_i]/[T]_0$, where $[T]$ means the concentration of TOPO and zero index in all cases means the initial concentration.

If our hypothesis that the preferential form obtained under low HP concentration ([HP]) is C_3, which gradually goes over to C_2 and C_1 under increasing excess of HP, then D should undergo substantial drop at first and then increase, limiting at the value of D_1.

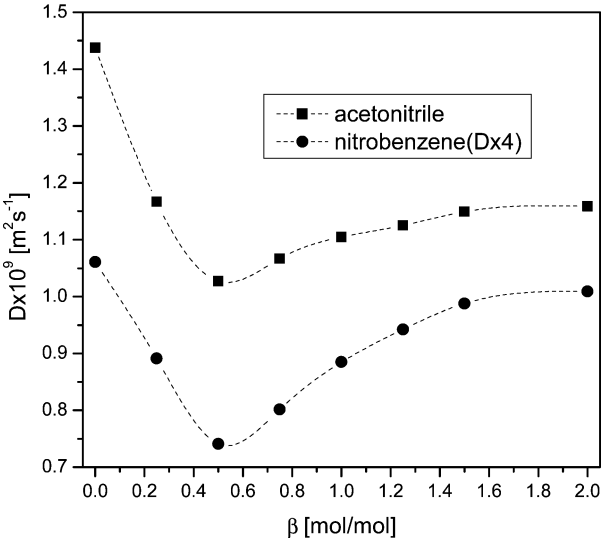

Figure 4. Self-diffusion coefficients D corresponding to signal 8 of TOPO in its mixtures with HP in the indicated solvents at 298 K (the values in nitrobenzene-d_5 are multiplied by 4 for better comparison and the experimental points are formally spline-connected).

SCHEME 2: Probable Structure of the Final Complex C_1 (R = *n*-Octyl)

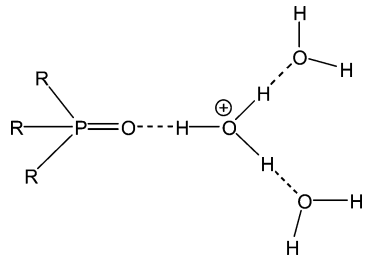

We measured D using signal 8 in the ^{1}H PGSTE NMR spectrum using linearly increasing field gradient g. All signal intensity decays were monoexponential in g^2 as expected. The results for increasing β obtained both in acetonitrile-d_3 and in nitrobenzene-d_5 are shown in Figure 4.

As expected, both dependences exhibit a significant drop at low β. The minima are not at $\beta = 0.33$ but somewhat higher, which shows that forms C_3 and C_2 must be coexistent in this concentration range. Also, D does not drop to a third of its original value D_0 as one would expect from the Stokes−Einstein expression $D = kT/6\pi\eta R_H$ but rather to its two-thirds. However, even if the species present at the minimum were exclusively C_3, there is no reason for believing the molecules of TOPO or C_3 to be spherical and their hydrodynamic radius R_H additive in the number of TOPO bound in the complex. The important feature we detect is that the prevailing species at low β is the largest one and the ones produced at larger values of β are progressively smaller limiting in one which remains unchanged even at very large β. It is reasonable to identify this final species with C_1.

We see, however, that D_1 is significantly lower than D_0, in particular in acetonitrile. Such change probably could not be due to attaching bare H_3O^+ to TOPO. It is probable that at least two other water molecules are attached to the complex in a manner suggested in Scheme 2.

Using ^{31}P NMR Chemical Shifts for the Study of Equilibria. In principle, the dependence of D on β from the previous paragraph could be used for analyzing the equilibria between TOPO and complexes C_3, C_2, and C_1. However, relative chemical shifts, in particular those of ^{31}P NMR signals, are much more reliable tools for this task: whereas the diffusion coefficient of a species can change due to labile binding of other components of the system, which in turn can depend on concentration, relative ^{31}P NMR chemical shift is primarily given by the change of electron density of the surroundings of the nucleus and thus to a number of positive ions attached in its vicinity. Formally, it is one-third of an elementary charge in C_3, one-half of it in C_2, and one whole charge in C_1. In reality, this quantity is somewhat lower in C_2 and especially C_1 because of the additional weaker binding of water molecules. Nonetheless, it is reasonable to expect C_1 to have the largest downfield shift compared to TOPO whereas C_2 and C_3 should have a progressively lower one.

Under fast exchange, it must hold (in direct analogy with eq 1) for the observed relative shift $\Delta\delta$:

$$\Delta\delta = \sum_i \alpha_i \Delta\delta_i \qquad (2)$$

where $\Delta\delta_i$ is the relative shift for the species C_i (i = 1, 2, 3). Equation 2 holds for any active nucleus of the system, but ^{31}P is the most appropriate in our case because the relative shifts are so large and thus very sensitive to the changes of the composition of the system.

Assuming that, besides free TOPO, we have only C_3, C_2, and C_1 in the system, the equilibria must obey the relations

$$K_i = \frac{[C_i]}{[T]^i[HP]} \qquad (3)$$

Equation 3 could be expressed more explicitly and combined with eq 2 to fit equilibrium constants to the experimental values of $\Delta\delta$. For this, we used the program[39] LETAGROP by Sillén and Warnquist, which optimizes the equilibrium constants using the experimental dependence of $\Delta\delta$ on β and the known value of $\Delta\delta_1$ and an initial guess of $\Delta\delta_2$ and $\Delta\delta_3$. Figure 5 shows experimental values of $\Delta\delta$ obtained in acetonitrile-d_3 and nitrobenzene-d_5 and the rather satisfying fitting curves obtained by this program. The optimized values of K_i are given in Table 1. Additionally, Figure 6 shows differential distributions of individual species in the same concentration range. Here, δ_{distr} means $\alpha_T = 1 - \sum_i \alpha_i$ for TOPO (curve 1) and α_i for all C_i (curves 2, 3, and 4). Using calculated values of α_i for each experimental point, we can use eq 2 to obtain the values of $\Delta\delta_i$. Having seven experimental points and three unknown $\Delta\delta_i$, the problem is overdetermined and has to be solved by linear optimization. The optimized values of $\Delta\delta_i$ reproduce the experimental values of $\Delta\delta$ within ±0.4 ppm are also given in Table 1. The match of calculated with experimental values of $\Delta\delta$ within at most 3% rel. strongly supports our model of the equilibria.

The values of $\Delta\delta_i$ almost linearly decrease with increasing number i of TOPO molecules in the complex, in accord with our assumption. When comparing individual K_i for the same medium, we have to bear in mind the different power of $[T]$ in their definition; one can say that they are roughly comparable. Also the values of K_1 and K_3 are expectedly comparable between the two media. The value of K_2 in nitrobenzene is surprisingly high; we have no solid hypothesis for this difference from acetonitrile.

NMR Study of the Dynamics of the System. As in the previous paragraph, we use ^{31}P NMR for the study of the dynamics utilizing as an advantage the existence of a single signal and the large relative chemical shifts between the exchanging sites. There certainly are many possible exchange

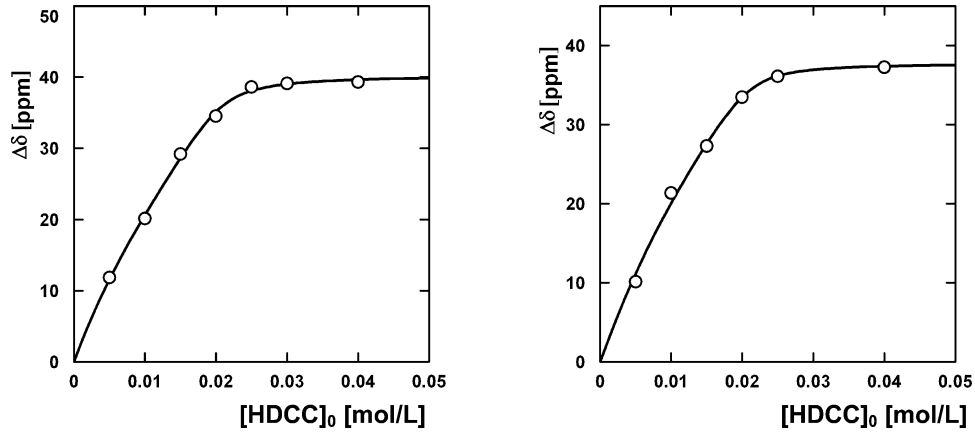

Figure 5. Experimental values of $\Delta\delta$ observed in acetonitrile-d_3 (left) and nitrobenzene-d_5 (right) at 296 K and their fitting by eq 3 using program LEGATROP.

TABLE 1: Optimized Values of $\Delta\delta_i$ (in ppm) and log K_i ($\pm$0.02) Obtained from the Experimental ^{31}P NMR Relative Shifts in the Region of β from 0 to 2

	acetonitrile		nitrobenzene	
i	log K_i	$\Delta\delta_i$	log K_i	$\Delta\delta_i$
1	3.63	39.35	3.91	38.37
2	4.67	29.51	6.04	28.47
3	7.23	19.72	7.92	18.63

processes going on in the system, and this study cannot hope to give a really exact picture of the dynamics involved. However, it can give a further support to our previous analysis.

As a slightly simplified picture of the overall exchange, we list six main processes E_{10} to E_{32} in Scheme 3, which lead to a change of TOPO chemical shift. Further complications of the scheme could be envisaged, for instance, exchange processes between HP bound in individual complexes and water, but these are not within our reach.

Unfortunately, not all TOPO−HP mixtures are suitable for the analysis of the dynamics. In particular, the most interesting instance ($\beta = 0.25, 0.75$) exhibits signals too broad for an exact T_2 measurement and also the half-widths of the signals do not give sufficiently precise results. Therefore, we have to use three slightly less informative cases ($\beta = 0.5, 1.25, 1.50$).

As is well-known, the dynamics of the system can be studied by the measurement of the transverse relaxation rate under varied interpulse delay t_p in the Carr−Purcell−Meiboom−Gill sequence (CPMG)[40] with a varied delay t_p between the π pulses. The actually measured relaxation rate $R_2(t_p)$ can be expressed[41] for two sites involved in unimolecular exchange as

$$R_2(t_p) = R_2^0 + p_1 p_2 \delta\omega^2 \tau_{ex}[1 - (\tau_{ex}/t_p)\tanh(t_p/\tau_{ex})] \quad (4)$$

where R_2^0 is the part of relaxation rate independent of exchange, p_1 and p_2 are the probabilities of finding the nucleus at the sites 1 and 2, respectively, $\delta\omega$ is the relative chemical shift between the two sites ($\delta\omega = 2\pi\Delta\delta$), and τ_{ex} is the correlation time of exchange. Assuming that $\tau_{ex} \ll t_p$, we use the approximation[42]

$$R_2(t_p) = \zeta - \xi/t_p \quad (5)$$

with

$$\zeta = R_2^0 + \xi/\tau_{ex} \quad (5a)$$

and

$$\xi = p_1 p_2 \delta\omega^2 {\tau_{ex}}^2 \quad (5b)$$

However, in the case of more exchange processes running at the same time, there are more contributions to R_2 and eqs 5a and 5b have to be modified accordingly. We suggest as a plausible approximation that the individual exchange processes are mutually independent as the exchanging molecules spend in their own form much more time than in the transformation during their exchange jumps. Under such an assumption, the part of transverse relaxation that is due to chemical exchange (which surely is a major par in our case) should be a sum of contributions of individual exchange processes. Let us define as p_{ij} the concentration-dependent probability of the reversible jump between sites i and j. Then eq 5a will be transformed to

$$\zeta = R_2^0 + \sum_{i,j} p_{ij} \delta\omega_{ij}^2 \tau_{ij} \quad (6a)$$

and eq 5b to

$$\xi = \sum_{i,j} p_{ij} \delta\omega_{ij}^2 \tau_{ij}^2 \quad (6b)$$

where $\delta\omega_{ij}$ is the *relative* chemical shift between the given sites (in rad/s) and τ_{ij} is the corresponding correlation time. In Scheme 2 there are expressed the probabilities p_{ij} for the main exchange processes. Here, α_T and α_i were defined above, α_H is the actual concentration of HP recalculated to the same scale. The actual values of p_{ij} for the chosen values of β are calculated from the corresponding α values obtained above for acetonitrile in Table 2; the values having numerical significance are in bold. As we can see, only exchange processes E_{10}, E_{21}, and E_{32} can have real significance in our measurements.

Considering this significance, let us rewrite eqs 6a and 6b into explicit forms:

$$\zeta = R_2^0 + \zeta_{10}\tau_{10} + \zeta_{21}\tau_{21} + \zeta_{32}\tau_{32} \quad (7a)$$

with

$$\zeta_{10} = p_{10}\delta\omega_1^2$$

$$\zeta_{21} = p_{21}(\delta\omega_1 - \delta\omega_2)^2$$

$$\zeta_{32} = p_{32}(\delta\omega_2 - \delta\omega_3)^2$$

and

$$\xi = \zeta_{10}{\tau_{10}}^2 + \zeta_{21}{\tau_{21}}^2 + \zeta_{32}{\tau_{32}}^2 \quad (7b)$$

where $\delta\omega_i = 2\pi\Delta\delta_i$, where $\Delta\delta_i$ shown in Table 1 in ppm must be expressed in hertz here (i.e., $\delta\omega_1 = 3.0025 \times 10^4$, $\delta\omega_2 = 2.2517 \times 10^4$, $\delta\omega_3 = 1.5047 \times 10^4$ rad/s). The fairly linear dependences of R_2 on $1/t_p$ for $\beta = 0.5$, 1.25, and 1.5 are given in Figure 7.

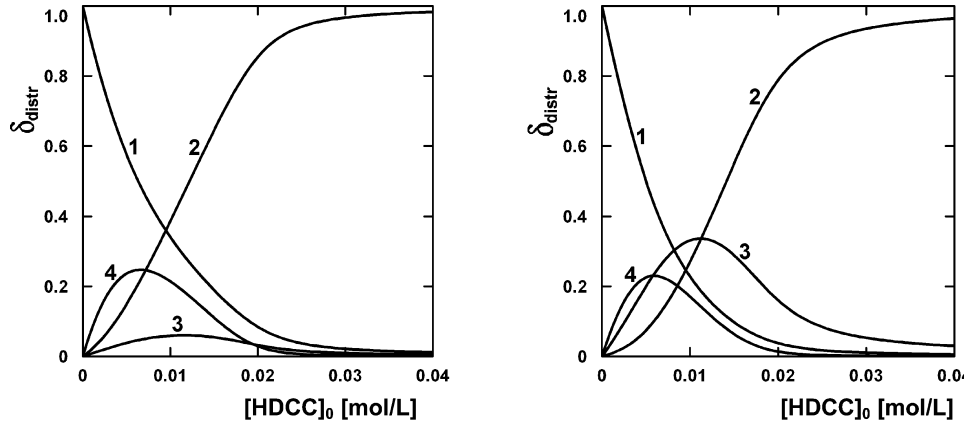

Figure 6. Calculated values of δ_{distr} for TOPO (1), TOPO·HP (2), $TOPO_2$·HP (3), and $TOPO_3$·HP (4) found in acetonitrile-d_3 (left) and nitrobenzene-d_5 (right) at 296 K.

SCHEME 3: Main Exchange Processes and Their Probability

E_{10}	TOPO+HP	$\overset{\tau_{10}}{\rightleftharpoons}$	C_1	$p_{10}=\alpha_T\alpha_H\alpha_1$
E_{20}	2TOPO+HP	$\overset{\tau_{20}}{\rightleftharpoons}$	C_2	$p_{20}=\alpha_T^2\alpha_H\alpha_2$
E_{30}	3TOPO+HP	$\overset{\tau_{30}}{\rightleftharpoons}$	C_3	$p_{30}=\alpha_T^3\alpha_H\alpha_3$
E_{21}	TOPO+C_1	$\overset{\tau_{21}}{\rightleftharpoons}$	C_2	$p_{21}=\alpha_T\alpha_1\alpha_2$
E_{31}	2TOPO+C_1	$\overset{\tau_{31}}{\rightleftharpoons}$	C_3	$p_{31}=\alpha_T^2\alpha_1\alpha_3$
E_{32}	TOPO+C_2	$\overset{\tau_{32}}{\rightleftharpoons}$	C_3	$p_{32}=\alpha_T\alpha_2\alpha_3$

Table 3 shows experimental values of the slopes ξ and abscissas ζ for these three dependences. It also shows the values of ζ_{ij} calculated from the values of p_{ij} and $\delta\omega$ obtained above. Using three variants of eq 7b with the incident values of ζ_{ij}, namely

$$5.416\times10^{-3}=0.998\times10^{6}\tau_{10}^{\,2}+0.438\times10^{6}\tau_{21}^{\,2}+0.236\times10^{6}\tau_{32}^{\,2} \quad (7b/1)$$

$$3.211\times10^{-4}=9.385\times10^{6}\tau_{10}^{\,2}+4.747\times10^{4}\tau_{21}^{\,2}+198.7\tau_{32}^{\,2} \quad (7b/2)$$

$$1.122\times10^{-4}=8.177\times10^{6}\tau_{10}^{\,2}+1.110\times10^{4}\tau_{21}^{\,2}+25.04\tau_{32}^{\,2} \quad (7b/3)$$

the following values of correlation times are obtained:

$$\tau_{10}=2.5\times10^{-6}\text{s},\ \tau_{21}=7.4\times10^{-5}\text{s},\ \tau_{32}=11.3\times10^{-5}\text{s}$$

Table 3 also shows the theoretical abscissas ζ_t calculated from these correlation times and ζ_{ij} using the formula

$$\zeta_t=\zeta_{10}\tau_{10}+\zeta_{21}\tau_{21}+\zeta_{32}\tau_{32} \quad (8)$$

where τ_{10}, τ_{21}, and τ_{32} are the experimental values obtained above. As expected, they are slightly lower than the experimental extrapolations (ζ_t does not include R_2^0) but otherwise in a very good accord with them.

The large difference between the slopes ξ for $\beta = 0.5$ and 1.25 or 1.5 is caused by the perceptibly larger relative contribution of the processes E_{21} and E_{32} given both by their probability (concentration of C_2 and C_3) and by the respective correlation times. The much shorter τ_{10} compared with τ_{21} or τ_{32} can be explained by the facility of approach between TOPO and HP molecules. The other two exchange processes always involve two large molecules and have to be slower even without respect to their concentration dependence.

The success of the analysis of the system dynamics also strongly supports our model of the TOPO−HP binding modes, which was originally derived only from the concentration dependence of the ^{31}P NMR chemical shift.

Theoretical Calculations. Both media in our experiments (acetonitrile, nitrobenzene) are relatively polar and thus certainly influence our reactants and products. There apparently is no really reliable and universal method of taking into account the polarity of the medium in precise DFT calculations. However, our experience with similar systems tells us that DFT calculations made in vacuo nonetheless give valuable structural information, often in very good agreement with experiments. This is particularly true if strong interactions between specific atomic groups of reacting molecules are examined such as in the present case.

We started our structure optimization with the molecule of TOPO itself. As there was some water present (about 1.2 mol/mol) in TOPO used for our experiments, we optimized also the structure of TOPO−monohydrate, which is graphically shown in Figure 8. As shown, the first water molecule is bound by a fairly strong hydrogen bond. Additional water molecules could be added on a near energy level, but this is not very important in the actual case. The calculated ^{31}P NMR chemical shift (relative to H_3PO_4) for the structure in Figure 8 is 38.3 ppm, which is in a fairly good agreement with the experimental value of 45.8 ppm in acetonitrile considering the scope of phosphorus chemical shifts.

Exploring now the complexes of TOPO with hydrated protons, we found three preferentially stable complexes, quite in accord with those supposed above. The optimal geometry of the first one, which corresponds to C_3 or $[3TOPO\cdot H_3O]^+$, is shown in Figure 9. The structure is mostly symmetric, with almost equally strong hydrogen bonds of H_3O^+ to the three P═O oxygen atoms. The calculated ^{31}P chemical shifts of the three phosphorus nuclei are 56.6, 57.8, and 57.9 ppm. It is reasonable (and in accord with NMR) to assume fast rotational averaging of the structure leading to the average shift 57.4 ppm, i.e., 19.1 ppm relative to TOPO, which is in excellent agreement with that derived from the experiments (19.7 ppm).

The optimized structure of the next complex corresponding to C_2 needs at least one additional water molecule to be stable. Schematically, it can be symbolized as $[2TOPO\cdot H_3O\cdot H_2O]^+$ and is shown in Figure 10. Somewhat surprisingly, the structure does not contain exactly the hydronium ion H_3O^+ as its building

TABLE 2: Values of Probability Coefficients of Individual Exchange Processes at Selected Values of β

β	p_{10}	p_{20}	p_{30}	p_{21}	p_{31}	p_{32}
0.50	$\mathbf{1.107 \times 10^{-3}}$	5.638×10^{-5}	6.848×10^{-5}	$\mathbf{7.787 \times 10^{-3}}$	1.354×10^{-4}	$\mathbf{4.242 \times 10^{-3}}$
1.25	$\mathbf{1.041 \times 10^{-2}}$	6.388×10^{-6}	9.348×10^{-8}	$\mathbf{8.431 \times 10^{-4}}$	2.738×10^{-6}	3.561×10^{-6}
1.50	$\mathbf{0.907 \times 10^{-2}}$	2.335×10^{-6}	1.186×10^{-8}	$\mathbf{1.972 \times 10^{-4}}$	4.835×10^{-7}	4.488×10^{-7}

block: one of its protons is pulled from its oxygen to a distance of a very strong hydrogen bond (1.38 Å) and is engaged in a P═O^+−H bond to one of the TOPO units.

The calculated ^{31}P chemical shifts for this structure are 55.0 and 79.7 ppm, respectively, which gives the average 67.4 ppm (assuming internal exchange again, in accord with NMR). This amounts to 29.1 ppm relatively to TOPO, which is again in excellent agreement with the value 29.5 ppm derived from NMR experiments.

Energetically quite near to this structure are its higher hydrates containing one or two additional water molecules. In these, H_3O^+ in the complex adopts a more symmetrical geometry and the calculated ^{31}P shifts are much closer to each other, differing from the above average in units of ppm.

The last energetically favorable structure in our calculations is that corresponding to C_1. It needs two additional water molecules for its stabilization, schematically [TOPO·H_3O·$2H_2O$]$^+$. The optimal geometry is shown in Figure 11. Again, one proton of H_3O^+ is pulled to a distance of even 1.44 Å from the hydronium ion oxygen by the P═O group, producing thus rather P−O−H^+ formation. The calculated ^{31}P NMR shift is 81.3 ppm, i.e., 43.0 ppm relative to TOPO. The slightly poorer agreement with experiment (39.4 ppm) can be explained by the fact that the experimental value was obtained under large excess of HP, i.e., water. The structure in Figure 11 allows further hydration without substantial gain of energy; in the higher-hydrated structures, the hydronium ion is more symmetric and the predicted position of the ^{31}P signal shifts near to the experimental one.

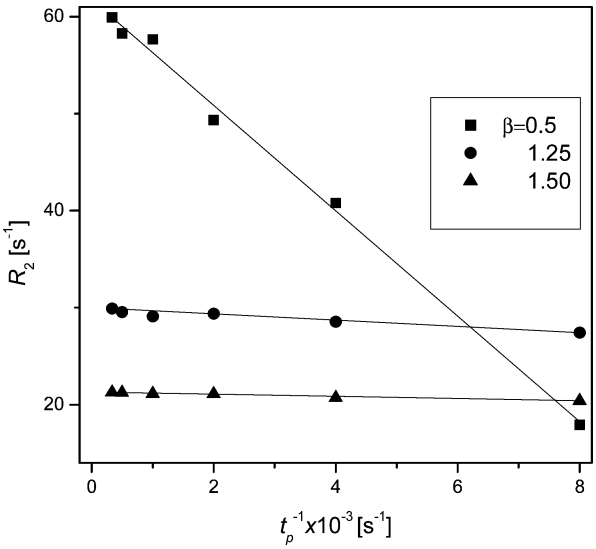

Figure 7. Experimental R_2 on t_p^{-1} dependences of the ^{31}P TOPO signal under indicated β = [HDCC]$_0$/[TOPO]$_0$ in acetonitrile-d_3 (296 K).

Conclusions

Using a combination of ^{1}H, ^{13}C, and ^{31}P NMR spectra, PFG diffusion measurements and relaxation studies with DFT theoretical calculations, the interaction of trioctylphosphine oxide (TOPO) with hydrated protons (HP) in acetonitrile-d_3 and nitrobenzene-d_5 was studied. HP were offered by hydrogen bis(1,2-dicarbollyl)cobaltate (HDCC) with 3.5 mol/mol of H_2O. The intensive complex-forming between TOPO and HP was proved by intensive relative shifts of respective signals in ^{1}H, ^{13}C, and ^{31}P NMR spectra. The formation of various types of the complex differing by relative TOPO content was demonstrated by the dependence of the apparent (averaged) diffusion coefficient (measured by ^{1}H PGSE NMR) on the molar ratio β = [HP]$_0$/[TOPO]$_0$. Both types of the complex and the corresponding stabilization constants K_i were derived by analyzing the dependence of the relative shift $\Delta\delta$ of the exchange-averaged ^{31}P NMR signal of TOPO on β using the computer program LETAGROP. The assumed presence of three types of complex with the schematic formula TOPO$_i$·HP (named C$_i$, i = 1, 2, 3) gave the best fit of the experimental $\Delta\delta/\beta$ dependences. The fitting values of log K_i were 3.63, 4.67, and 7.23 in acetonitrile and 3.91, 6.04, and 7.92 in nitrobenzene for C_1, C_2, and C_3, respectively. The simultaneously obtained respective ^{31}P relative shifts $\Delta\delta_i$ are 39.35, 29.51, and 19.72 ppm in acetonitrile and 38.37, 28.47, and 18.63 ppm in nitrobenzene.

Although three complexes with different relative shifts $\Delta\delta_i$ are present at most values of β, only a single signal was observed in ^{31}P NMR spectra and likewise, for the nuclei of the same type, in ^{1}H and ^{13}C NMR spectra, indicating thus fast exchange between C_1, C_2, and C_3. We performed an analysis of this exchange dynamics partly for its own sake and partly as a double check of the consistency of the previous analysis of the equilibria. For it, we used a method of measuring the dependence of the transverse relaxation rate R_2 of the ^{31}P NMR signal on the inverse of the time delay t_p between the π pulses in the Carr−Purcell−Meiboom−Gill (CPMG) pulse sequence in the mixtures with β = 0.5, 1.25, and 1.5 (leaving out the cases with too broad signals where the precision of measurement was low). As we suggest in the theory of these experiments, the slopes and abscissas of the resulting plots depend on the correlation times τ_{ij} of exchange between states i and j but also on the values of the relative shifts $\Delta\delta_i$ and the relative populations α_i = [C$_i$]/[TOPO]$_0$.

The program LEGATROP used in analyzing the equilibria also gave the possibility of calculating the values of both $\Delta\delta_i$

TABLE 3: Experimental Values of Slopes ξ (Dimensionless) and Abscissas ζ (in s^{-1}) of the R_2 on t_p^{-1} dependences of the ^{31}P NMR TOPO Signal under Indicated β = [HDCC]$_0$/[TOPO]$_0$ in Acetonitrile-d_3 (296 K) Together with the Calculated Factors ζ_{ij} (s^{-2}) and the Theoretical Values of ζ_t (s^{-1})

β	ξ	ζ	ζ_{10}	ζ_{21}	ζ_{32}	ζ_t
0.50	5.433×10^{-3}	62.23	0.998×10^6	0.438×10^6	0.236×10^6	61.72
1.25	3.236×10^{-4}	31.23	9.9385×10^6	4.747×10^4	198.7	30.01
1.50	1.121×10^{-4}	22.05	8.177×10^6	1.110×10^4	25.04	21.31

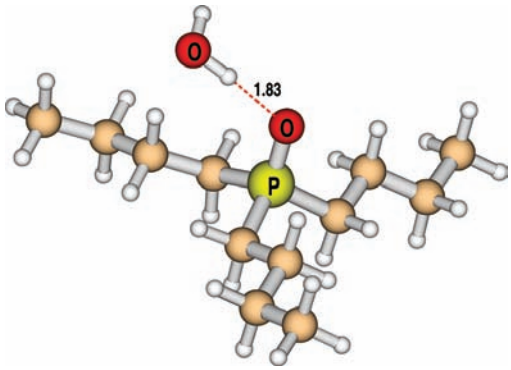

Figure 8. Optimized structure of the monohydrated TOPO molecule (B3LYP/6-31G(d)).

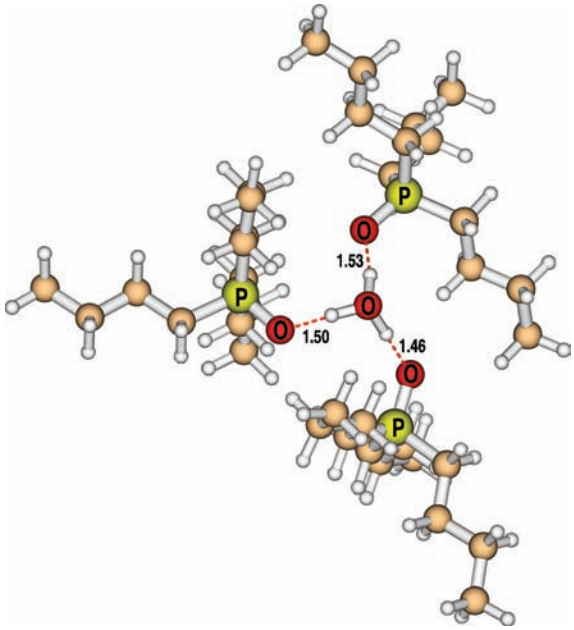

Figure 9. Optimized structure of the C_3 complex (B3LYP/6-31G(d)).

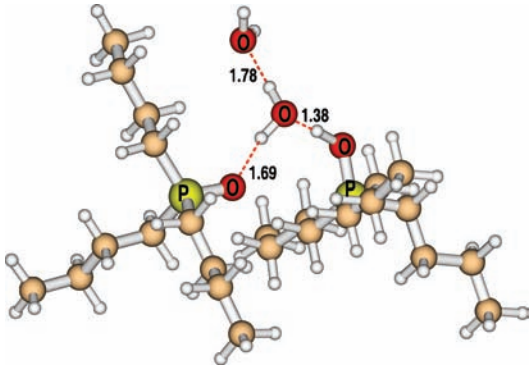

Figure 10. Optimized structure of the monohydrated C_2 complex (B3LYP/6-31G(d)).

and α_i. Statistical analysis based on the values of α_i shows that only three exchange processes can substantially influence the R_2 dependence on t_p^{-1} at the chosen values of β, namely, $C_1 \leftrightarrow$ TOPO (E10), $C_2 \leftrightarrow C_1$ (E21), and $C_3 \leftrightarrow C_2$ (E32). For these, the respective exchange correlation times $\tau_{10} = 2.5 \times 10^{-6}$, $\tau_{21} = 7.4 \times 10^{-5}$, and $\tau_{32} = 11.3 \times 10^{-5}$ s were calculated from the three slopes of the R_2/t_p^{-1} dependences. The abscissas calculated from these correlation times using the known values of $\Delta\delta_i$ and α_i were very near to the experimental ones which proved the performed analysis of dynamics (and thus, indirectly, the analysis of equilibria) to be consistent.

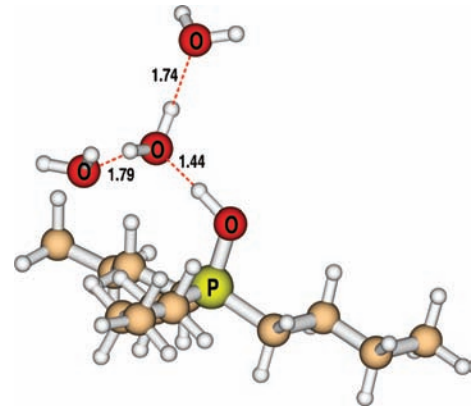

Figure 11. Optimized structure of the dihydrated C_1 complex (B3LYP/6-31G(d)).

Theoretical DFT calculations of the structures showed that the complexes C_3, C_2, and C_1 are the most stable variants of the possible complexes. Schematically, their composition can be expressed as $[3TOPO \cdot H_3O]^+$, $[2TOPO \cdot H_3O \cdot H_2O]^+$, and $[TOPO \cdot H_3O \cdot 2H_2O]^+$; i.e., additional water molecules are needed for the stabilization of C_2 and C_1. However, the hydronium ion H_3O^+ appears not to be really present as a building block of the latter two complexes unless they are hydrated to a higher degree. In their basic form corresponding to the schematic compositions shown above, one proton is pulled from H_3O^+ to one of the P═O groups, forming thus a grouping that could be symbolized as $P{-}O{-}H^+ \cdots H_2O$. In C_2, the two P═O groups are rapidly exchanged in this grouping so that no difference between the two phosphorus nuclei is observed by NMR.

The relative ^{31}P NMR shifts theoretically calculated for the optimized structures of C_1, C_2, and C_3 are 43.0, 29.1, and 19.1 ppm, respectively, which is in very good agreement with the experimentally observed values 39.35, 29.51, and 19.72 ppm.

Acknowledgment. This work was supported by the Grant Agency of the Czech Republic, Project 203/09/1478, and the Czech Ministry of Education, Youth and Sports, Projects MSM 4977751303 and MSM 6046137307.

References and Notes

(1) Gutsche, C. D. *Calixarenes Revisited*; The Royal Society of Chemistry: Cambridge, U.K., 1998.
(2) Böhmer, V. *Angew. Chem., Int. Ed. Engl.* **1995**, *34*, 713.
(3) Arduini, A.; Pochini, A.; Reverberi, S.; Ungaro, R. *Tetrahedron* **1986**, *42*, 2089.
(4) Arduini, A.; Ghidini, E.; Pochini, A.; Ungaro, R.; Andreetti, G. D.; Calestani, G.; Ugozzoli, F. *J. Inclusion Phenom.* **1988**, *6*, 119.
(5) Arnaud-Neu, F.; Collins, E. M.; Deasy, M.; Ferguson, G.; Harris, S. J.; Kaitner, B.; Lough, A. J.; McKervey, M. A.; Marques, E.; Ruhl, B. L.; Schwing-Weill, M. J.; Seward, E. M. *J. Am. Chem. Soc.* **1989**, *111*, 8681.
(6) Arnaud-Neu, F.; Barrett, G.; Harris, S. J.; Owens, M.; McKervey, M. A.; Schwing-Weill, M. J.; Schwinté, P. *Inorg. Chem.* **1993**, *32*, 2644.
(7) Ohto, K.; Murakami, E.; Shinohara, T.; Shiratsuchi, K.; Inoue, K.; Iwasaki, M. *Anal. Chim. Acta* **1997**, *341*, 275.
(8) Ye, Z.; He, W.; Shi, X.; Zhu, L. *J. Coord. Chem.* **2001**, *54*, 105.
(9) Danil de Namor, A. F.; Chahine, S.; Kowalska, D.; Castellano, E. E.; Piro, O. E. *J. Am. Chem. Soc.* **2002**, *124*, 12824.
(10) Marcos, P. M.; Ascenso, J. R.; Segurado, M. A. P.; Pereira, J. L. C. *J. Inclusion Phenom.* **2002**, *42*, 281.
(11) Marcos, P. M.; Félix, S.; Ascenso, J. R.; Segurado, M. A. P.; Pereira, J. L. C.; Khazaeli-Parsa, P.; Hubscher-Bruder, V.; Arnaud-Neu, F. *New J. Chem.* **2004**, *28*, 748.
(12) Steed, J. W. *Coord. Chem. Rev.* **2001**, *215*, 171.

(13) Steed, J. W.; Sakellariou, E.; Junk, P. C.; Smith, M. *Chem. - Eur. J.* **2001**, *7*, 1240.
(14) Lämsä, M.; Pursiainen, J.; Rissanen, K.; Huuskonen, J. *Acta Chem. Scand.* **1998**, *52*, 563.
(15) Kříž, J.; Dybal, J.; Makrlík, E.; Vaňura, P.; Lang, J. *Supramol. Chem.* **2007**, *19* (6), 419.
(16) Kříž, J.; Dybal, J.; Makrlík, E.; Vaňura, P. *Supramol. Chem.* **2008**, *20* (4), 387.
(17) Kříž, J.; Dybal, J.; Makrlík, E.; Budka, J. *Magnet. Reson. Chem.* **2008**, *46*, 235.
(18) Kříž, J.; Dybal, J.; Makrlík, E.; Budka, J.; Vaňura, P. *Monatsh. Chem.* **2007**, *138*, 735.
(19) Kříž, J.; Dybal, J.; Makrlík, E.; Budka, J.; Vaňura, P. *Supramol. Chem.* **2008**, *20* (5), 487.
(20) Calleja, M.; Johnson, K.; Belcher, W. J.; Steed, J. W. *Inorg. Chem.* **2001**, *40*, 4978.
(21) Bühl, M.; Wipff, G. *J. Am. Chem. Soc.* **2002**, *124*, 4473.
(22) Varnek, A.; Wipff, G.; Famulari, A.; Raimondi, M.; Vorob'eva, T.; Stoyanov, E. S. *J. Chem. Soc., Perkin Trans.* **2002**, *2*, 887.
(23) Stoyanov, E. S.; Reed, C. A. *J. Phys. Chem. A* **2004**, *108*, 907.
(24) Bühl, M.; Ludwig, R.; Schurhammer, R.; Wipff, G. *J. Phys. Chem. A* **2004**, *108*, 11463.
(25) Junk, P. C. *New J. Chem.* **2008**, *32*, 76.
(26) Kříž, J.; Dybal, J.; Makrlík, E.; Budka, J. *J. Phys. Chem. A* **2008**, *112*, 10236–10243.
(27) Kříž, J.; Dybal, J.; Budka, J.; Makrlík, E. *Magn. Reson. Chem.* **2008**, *46*, 1015–1024.
(28) Shigemat, T.; Matsui, M.; Wake, R. *Anal. Chim. Acta* **1969**, *1*, 101.
(29) Petkovic, D. M.; Ruvarac, A. L.; Konstant, J. M. *J. Chem. Soc., Dalton Trans.* **1973**, *16*, 1649.
(30) Moriya, H.; Sekine, T. *Bull. Chem. Soc. Jpn.* **1972**, *45*, 1626.
(31) Machanda, V. K.; Chander, K.; Sing, N. P. *J. Inorg. Nucl. Chem.* **1977**, *39*, 1039.
(32) Ohashi, K.; Yoshikawa, S.; Akutsu, B. *Anal. Sci.* **1990**, *6*, 827.
(33) Rao, R. R.; Chatt, A. *Radiochim. Acta* **1991**, *54*, 181.
(34) Narbutt, J.; Krejzler, J. *Inorg. Chim. Acta* **1999**, *286*, 175.
(35) Brennetot, R.; Georges, J. *Spectrochim. Acta A* **2000**, *56*, 703.
(36) Arnaud, N.; Georges, J. *Spectrochim. Acta A* **2003**, *59*, 1829.
(37) Oliva, M. D. A.; Olsina, R. A.; Masi, A. N. *Analyst* **2005**, *130*, 1312.
(38) Kříž, J.; Dybal, J.; Makrlík, E. *Biopolymers* **2006**, *82*, 536.
(39) Sillén, L. G.; Warnquist, B. *Ark. Kemi* **1969**, *31*, 315.
(40) Meiboom, S.; Gill, D. *Rev. Sci. Instrum.* **1958**, *29*, 688.
(41) Luz, L.; Meiboom, S. *J. Chem. Phys.* **1963**, *39*, 366.
(42) Canet, D.; Robert, J. B. In *Dynamics of Solutions and Fluid Mixtures by NMR*; Delpuech, J. J., Ed.); Wiley: Chichester, U.K., 1995; p 127.
(43) Stejskal, E. O.; Tanner, J. E. *J. Chem. Phys.* **1965**, *42*, 288.
(44) Tanner, J. E. *J. Chem. Phys.* **1970**, *52*, 2523.
(45) Frisch, M. J.; Trucks, G. W.; Schlegel, H. B.; Scuseria, G. E.; Robb, M. A.; Cheeseman, J. R.; Montgomery J. A., Jr.; Vreven, T.; Kudin, K. N.; Burant, J. C.; Millam, J. M.; Iyengar, S. S.; Tomasi, J.; Barone, V.; Mennucci, B.; Cossi, M.; Scalmani, G.; Rega, N.; Petersson, G. A.; Nakatsuji, H.; Hada, M.; Ehara, M.; Toyota, K.; Fukuda, R.; Hasegawa, J.; Ishida, M.; Nakajima, T.; Honda, Y.; Kitao, O.; Nakai, H.; Klene, M.; Li, X.; Knox, J. E.; Hratchian, H. P.; Cross, J. B.; Bakken, V.; Adamo, C.; Jaramillo, J.; Gomperts, R.; Stratmann, R. E.; Yazyev, O.; Austin, A. J.; Cammi, R.; Pomelli, C.; Ochterski, J. W.; Ayala, P. Y.; Morokuma, K.; Voth, G. A.; Salvador, P.; Dannenberg, J. J.; Zakrzewski, V. G.; Dapprich, S.; Daniels, A. D.; Strain, M. C.; Farkas, O.; Malick, D. K.; Rabuck, A. D.; Raghavachari, K.; Foresman, J. B.; Ortiz, J. V.; Cui, Q.; Baboul, A. G.; Clifford, S.; Cioslowski, J.; Stefanov, B. B.; Liu, G.; Liashenko, A.; Piskorz, P.; Komaromi, I.; Martin, R. L.; Fox, D. J.; Keith, T.; Al Laham, M. A.; Peng, C. Y.; Nanayakkara, A.; Challacombe, M.; Gill, P. M. W.; Johnson, B.; Chen, W.; Wong, M. W.; Gonzalez, C.; Pople, J. A. *Gaussian 03*, revision C.02; Gaussian, Inc.: Wallingford CT, 2004.

JP9012575